Preprints of the 21st IFAC World Congress (Virtual)
Berlin, Germany, July 12-17, 2020

DNN projectional observer for advanced ozonation systems of complex contaminants mixtures ⋆

Olga Andrianova *, **Tatyana Poznyak** **,
Alexander Poznyak *** and **Isaac Chairez** ****

* *National Research Univ. Higher School of Economics and ICS RAS, Russia*
** *SEPI, ESIQIE, Instituto Politecnico Nacional, Mexico*
*** *Automatic Control Department, CINVESTAV-IPN, Mexico*
**** *Bioprocesses Department, UPIBI, Instituto Politecnico Nacional, Mexico*

Abstract: The aim of this study is to provide a class of state observers, based on differential neural networks, to approximate a class of advanced oxidation systems, based on the application of ozone high oxidant power and catalyst (the named catalytic ozonation). The study considers the design of a state observer for uncertain systems with the restrictions of the ozonation system, including the positivity of the states, as well as the control action. The observer includes a projection operator which is motivated by the state constraints. The learning laws of the proposed differential neural networks are obtained using a class of controlled state restricted Lyapunov functions. The detailed stability analysis proves the input to state stability with respect to the modeling error, as well as the bounded uncertainties of the ozonation system. The experimental confirmation of the state estimation is also presented. The experimental case considers the ozonation of a toxic organic contaminant (therephtalic acid) which is a regular pollutant of the plastic industry wastewater.

Keywords: Catalytic ozonation; Adaptive state observer, Differential neural network; State restrictions; Projection operators.

1. INTRODUCTION

There is a wide variety of inorganic materials which have been tested as catalysts in heterogeneous catalytic ozonation systems. Such material include Titanium oxide (TiO_2), supported metals (Ni, Mo, Ce, etc), and unsupported or supported metal oxides, which are regular catalysts. In the last few decades, the catalytic ozonation reaction has been explained by two main reaction mechanisms Rodríguez et al. (2013). The first of these mechanisms assumes that organics, reacting with ozone, are adsorbed on the catalyst surface and then, decomposed by either ozone or the produced hydroxyl radicals Guan et al. (2013). The second of the proposed mechanisms supposes that both ozone and organic compounds are simultaneously adsorbed on the catalyst surface, and then the organic derivative products (formed by the redox process) are oxidized by both ozone and the produced hydroxyl radicals Nawrocki and Kasprzyk-Hordern (2010). In consequence, the catalytic ozonation is considered as a non selective process; however, the chemical structure of the initial compound is a main factor which may define its interactions with the catalyst along the ozonation. With the aim of suggesting a suitable method to apply the catalytic ozonation system in real treatment plants, it is necessary to optimize the use of the catalyst Wang and Bai (2017).

One of the possible options to justify the application of the catalytic ozonation is supporting the catalyst on solid inert support forming thin films Li et al. (2003). These catalytic films do not require filtering the liquid and may preserve the catalyst in the reactor and promote its re-use for several reaction rounds. Catalytic ozonation can be considered as a promising method to decompose toxic organics, which cannot be decomposed by other methods. However, the enhancement of the catalytic ozonation efficiency requires the application of diverse strategies, including the adjustment of the operating conditions for the ozonation system. For exerting such optimization, it may be necessary to use a suitable model of the catalytic ozonation system. The development of such a model is a complex task considering the high number of reactions between the organic compounds, ozone, the catalyst and the formed byproducts. An alternative is using adaptive approximate representations of the ozonation model. Adaptive non-parametric models can offer the options of either characterizing the catalyzed ozonation reaction or adjusting the operation conditions of catalytic ozonation implementing a class of adaptive control based on the approximated model. This is one of the main motivations for implementing novel techniques of non-parametric modelling.

Differential neural networks (DNNs) have proven to be efficient approximate representations of systems with uncertain models Poznyak et al. (2001); Wu (1998). DNNs, also known as Auto Associative or Feedback Networks, define a class of artificial neural networks, where the connections between units and output form a directed cycle. This creates an internal state of the network, yielding the exhibition of dynamic temporal-dependent behavior Chairez (2009). DNNs can use their internal memory to process arbitrary sequences of inputs. In DNN, the signal travels in both forward and backward directions, by introducing loops in the network architecture or topology. The potential application of DNN, to obtain approximate models

⋆ This work is partially supported by CPER DATA "ControlHub", ANR DIGITSLID 18-CE40-0008, the Government of Russian Federation (Grant 08-08), the Ministry of Education and Science of Russian Federation (Project 14.Z50.31.0031), and Russian Foundation for Basic Research (Project No. 19-08-00535).

of the catalytic ozonation, must consider several challenging aspects, such as the limited available information, to obtain the approximate model, the positive nature of all the states, which describe the catalytic ozonation system, and the large number of states needed to obtain a usable DNN-based model of the system Poznyak et al. (2019a); Hassani et al. (2018).

The potential application of DNN on estimating the evolution of variables which define catalytic ozonation must consider one of their principal characteristics: the positiveness of such states. Therefore, this study introduces a method for gathering the modeling abilities of DNN and projector operator which forces the estimated model corresponds the chemical nature of catalytic ozonation.

The main contributions of this study are: a) the development of an approximate model for a class of catalytic ozonation systems, considering that the catalyst is supported in solid supports and forming thin films, b) the development of a software sensor, to approximate the catalytic ozonation dynamic behavior, considering the positiveness of all the states, and c) an experimental confirmation of the software sensor application to recover the approximate model of the catalytic ozonation of 4-chlorophenol ($4-CPh$) and 4-phenolsulfonic acid ($4-PSA$) using CeO_2 as the catalyst. The rest of this manuscript is organized as follows. Section II presents the development of an approximate model of the catalytic ozonation system including the design of the DNN based state observer. Section III describes the design of the learning law which is applicable to the class of developed software sensors. Section IV details the application of the DNN state observer to reproduce the dynamics of a catalytic ozonation of $4-CPh$ as well as $4-PSA$. Section V closes the study with some final remarks.

2. ADAPTIVE STATE OBSERVER FOR OZONATION SYSTEMS

This section describes the design of the suggested state observer. The system to be approximated is described by the vector of variables $x=[c^g, Q, OH, c_1, c_{11}, ..., c_{1n}]$, where the sense of all states is defined as follows: the catalytic ozonation model may include two sections: a) the first one formed by a basic nominal model, that contains the mass-transfer of ozone and its reaction with contaminants, and b) an uncertain section that includes all the non-modeled reactions taking place. The ozone dissolved in the aqueous phase (Q, $mole$) is transferred from the gaseous phase (with a given ozone concentration c^g), obeying the double layer theory. This Q is consumed by the reaction with the contaminants, as well as the corresponding by-products and it is also used to produce hydroxyl radicals. The initial contaminant concentration is represented by c_1, $mole\cdot L^{-1}$ and its byproducts concentrations are given by $\left(c_{1i},\ mole\cdot L^{-1},\ i\in[1,N]\right)$. All these organics are decomposed by the reaction with the dissolved ozone as well as with the hydroxyl radicals (OH, $mole\cdot L^{-1}$). These radicals are produced from the self-decomposition of dissolved ozone, as well as by the action of the catalyst.

With the aim of providing a suitable approximate model of the catalytic ozonation system, let's propose a general class of dynamic systems with uncertain dynamics that can represent the time variation of x.

2.1 Uncertain dynamic system

Assume that the catalytic ozonation system can be represented by an uncertain non-negative ODE given by:

$$\frac{d}{dt}x(t)=f(x(t),u(t),t),\quad x(0)=x_0,\ \|x_0\|<\infty. \tag{1}$$

The output $y=c^g$ is described by

$$y(t)=Cx(t)+\nu(t), \tag{2}$$

then $C=[\,1\ 0\ \cdots\ 0\,]$. In view of the nature of the variables in x, the state has non-negative bounded components

$$0\le x_i\le x_i^+,\ i=1,...,n,\ \left(x^+\right)^2:=\sum_{i=1}^{n}\left(x_i^+\right)^2. \tag{3}$$

The variable $u(t)\in U_{adm}\subset\mathbb{R}^m$, $m<n$ may describe a possible control action, which must satisfy boundedness conditions on state components (3). Variable $\nu(t)\in\mathbb{R}^q$ defines bounded noises affecting the output.

2.2 Main assumptions

The principal assumptions considered in this study are:

(1) The dimension of the state n is known.
(2) The admissible controls $u(t)$ and noises $\nu(t)$ are within the following bounds (the bounds u_+ and ν_+ are known), i.e.,
$$U_{adm}=\left\{u:\|u\|^2\le u_+^2<\infty\right\} \tag{4}$$
and
$$\|\nu(t)\|\le\nu_+<\infty. \tag{5}$$
(3) The mapping $f:\mathbb{R}^n\times\mathbb{R}^m\times\mathbb{R}\longrightarrow\mathbb{R}^n$ is unknown, but locally Lipschitz.
(4) The upper bounds x_i^+ in (3) are known and constant.
(5) There is a Hurwitz matrix $A\in\mathbb{R}^{n\times n}$ (maybe unknown) such that $\forall\ x\in\mathbb{R}^n$, all $u(t)\in U_{adm}$ and all $t\ge 0$ the following property holds (satisfying (3)):
$$\|\delta_A f(x,u,t)\|^2\le\theta, \tag{6}$$
where
$$\delta_A f(x,u,t):=f(x,u,t)-Ax. \tag{7}$$

3. DNN OBSERVER FOR POSITIVE UNCERTAIN SYSTEMS

Consider the DNN observer (DNNO) satisfying the following structure: [1]

$$\left.\begin{array}{c}\frac{d}{dt}\bar{x}(t)=A\hat{x}(t)+W_1(t)\Psi_1(\hat{x}(t))+\\ W_2(t)\Psi_2(\hat{x}(t))u(t)+L\left[y(t)-C\hat{x}(t)\right],\\ \\ \hat{x}(t)=\Pi_X\left\{\bar{x}(t)\right\}.\end{array}\right\} \tag{8}$$

Here $\Pi_X\{\bar{x}\}$ defines the projection operator as

$$\Pi_X\{\bar{x}\}=\left\{\mathrm{sat}_1(\bar{x}_1),...,\mathrm{sat}_n(\bar{x}_n)\right\},$$
$$\mathrm{sat}_i(\bar{x}_i)=\begin{cases}0 & if\quad \bar{x}_i<0\\ \bar{x}_i & if\ \bar{x}_i\in\left[0,x_i^+\right]\\ x_i^+ & if\quad x_i^+<\bar{x}_i.\end{cases} \tag{9}$$

The vector $\hat{x}(t)\in\mathbb{R}^n$ is the state estimation vector, $\bar{x}(t)\in\mathbb{R}^n$ is an intermediate auxiliary variable, $W_1(t)\in\mathbb{R}^{n\times l}$ and $W_2(t)\in\mathbb{R}^{n\times s}$ are the time varying weighting matrices which

[1] The similar DNNO structure without the projection component was suggested in Poznyak et al. (2001) and Poznyak et al. (2019b).

must be adjusted during the training procedure, $\Psi_1(x) \in \mathbb{R}^l$ and $\Psi_2(x) \in \mathbb{R}^{s\times m}$ are given activation vectorial and matrix functions. These activations have sigmoidal components, which satisfy the following structure:

$$\left.\begin{array}{l} \Psi_{1,r}(x) = \dfrac{a_r}{1+b_r e^{\left(-c_r^\top x\right)}} \\ \Psi_{2,rp}(x) = \dfrac{a_{rp}}{1+b_{rp} e^{\left(-c_{rp}^\top x\right)}} \\ a_r,\ a_{rp},\ b_r,\ b_{rp} > 0, \\ c_r \in \mathbb{R},\ c_{rp} \in \mathbb{R}^n \end{array}\right\} \tag{10}$$

Evidently, $\Psi_1(x)$ and $\Psi_2(x)$ are bounded:

$\|\Psi_1(x)\| \le L_{\Psi_1}^+$, $\|\Psi_2(x)u\| \le Lu_+$.

Notice that, in view of the projection operator property (9), vectors $\hat{x}(t)$ and $\bar{x}(t)$ satisfy the inequality

$$\|\hat{x}(t) - x(t)\| \le \|\bar{x}(t) - x(t)\|. \tag{11}$$

4. LEARNING LAWS

Assume that the right-hand side of the system with uncertain dynamics (1) can be represented as

$$\frac{d}{dt}x(t) = Ax(t) + \mathring{W}_1\Psi_1(x(t)) + \mathring{W}_2\Psi_2(x(t))u(t),$$

let's consider the following learning laws for the DNNO weights on-line adjustment:

$$\begin{array}{c} \dot{W}_1(t) = -\dfrac{\alpha}{2}\tilde{W}_1(t) - \\ \dfrac{1}{k_{w,1}} P\left(C^\top C + \delta I\right)^{-1} C^\top e \Psi_1^\top(\hat{x}(t)) \\ -\dfrac{1}{2k_{w,1}} P\Lambda_w^{-1} P\tilde{W}_1(t)\Psi_1(\hat{x}(t))\Psi_1^\top(\hat{x}(t)) \end{array} \tag{12}$$

$$\begin{array}{c} \dot{W}_2(t) = -\dfrac{\alpha}{2}\tilde{W}_2(t) - \\ \dfrac{1}{k_{w,2}} P\left(C^\top C + \delta I\right)^{-1} C^\top e(t) u^\top(t) \Psi_2^\top(\hat{x}(t)) \\ -\dfrac{1}{2k_{w,2}} P\Lambda_w^{-1} P\tilde{W}_2(t)\Psi_2(\hat{x}(t))u(t)u^\top(t)\Psi_2^\top(\hat{x}(t)). \end{array}$$

Here $\tilde{W}_i(t) := W_i(t) - \mathring{W}_i$ $(i = 1,2)$; α, $k_{w,1}$, $k_{w,2}$, δ are positive parameters, $\Lambda_w \in R^{n\times n}$ is any positive definite matrix, and

$$e(t) := C\bar{x}(t) - y(t). \tag{13}$$

Matrices $\mathring{W}_1$, $\mathring{W}_2$, L, P, as well as the parameters α, δ, participating in (12), will be obtained using an optimization procedure based on the theory of matrix inequalities.

5. MAIN RESULT ON THE QUALITY OF THE SUGGESTED PROJECTIONAL DNNO

Theorem 1. *Consider the projectional DNNO (8) supplied by Learning Laws (12), where all matrix, vector and scalar parameters are fixed. If, for the given DNNO, there exist positive definite (symmetric) matrices $P \in \mathbb{R}^{n\times n}$, $L \in \mathbb{R}^{n\times q}$, $A \in \mathbb{R}^{n\times n}$, $\mathring{W}_1 \in \mathbb{R}^{n\times l}$, $\mathring{W}_2 \in \mathbb{R}^{n\times s}$, and a positive scalar parameter ε such that the following matrix inequality holds:*

$$\begin{array}{c} H\left(P, L, A, \mathring{W}_1, \mathring{W}_2 \mid \alpha, \varepsilon, \delta\right) := \\ \begin{pmatrix} H_{11} & -P \\ -P & -\varepsilon I_{n\times n} \end{pmatrix} < 0, \\ H_{11} = P\left(A - LC + \dfrac{\alpha}{2}I\right) + \left(A - LC + \dfrac{\alpha}{2}I\right)^\top P + \\ P\left[(A\text{-}LC)\Lambda_x^{-1}(A\text{-}LC)^\top + L\Lambda_L^{-1}L^\top\right]P + \\ P\left(\mathring{W}_1\Lambda_{\mathring{w}_1}^{-1}\mathring{W}_1^\top + \mathring{W}_2\Lambda_{\mathring{w}_2}^{-1}\mathring{W}_2^\top\right)P + \\ 2\|\Lambda_x\| I_{n\times n} + \delta^2\left(C^\top C + \delta I\right)^{-1}\Lambda_w\left(C^\top C + \delta I_{n\times n}\right)^{-1}, \end{array} \tag{14}$$

then all possible trajectories of the state estimation error $\hat{\Delta}(t) := \hat{x}(t) - x(t)$ asymptotically arrive (approach) to the centered attractive ellipsoid $\mathscr{E}(P_{attr})$ with the ellipsoidal matrix $P_{attr} \in \mathbb{R}^{n\times n}$, fulfilling

$$\limsup_{t\to\infty} \hat{\Delta}^\top(t) P_{attr} \hat{\Delta}(t) \le 1 \tag{15}$$

where

$$P_{attr} = \frac{\alpha}{\beta}P \tag{16}$$

with

$$\begin{array}{l} \beta = 2\|\Lambda_x\|\left(\sum\limits_{i=1}^{n}\left(x_i^+\right)^2 + \left(x^+\right)^2\right) + \|\Lambda_L\|\nu_+^2 + \varepsilon\theta + \\ \left\|\Lambda_{\mathring{w}_1}\right\|\left(L_{\Psi_1}^+\right)^2 + \left\|\Lambda_{\mathring{w}_2}\right\|\left(L_{\Psi_2}^+ u_+\right)^2 + \\ \left\|C\left(C^\top C + \delta I\right)^{-1}\Lambda_w\left(C^\top C + \delta I\right)^{-1}C^\top\right\|(\nu_+)^2. \end{array} \tag{17}$$

Here matrices $\Lambda_x \in \mathbb{R}^{n\times n}$, $\Lambda_L \in \mathbb{R}^{q\times q}$, $\Lambda_w \in \mathbb{R}^{n\times n}$, $\Lambda_{\mathring{w}_1} \in \mathbb{R}^{l\times l}$, $\Lambda_{\mathring{w}_2} \in \mathbb{R}^{s\times s}$ are known. A brief summary of the proof of this theorem is given in Appendix.

5.1 Minimization of Attractive Ellipsoid

The best parameters selection is realized by the solution of the following constrain optimization problem with LMI's:

$$\begin{array}{rc} \mathrm{tr}P_{attr} = \dfrac{\alpha}{\beta}\mathrm{tr}P \to & \sup \\ & P > 0, Z_1, Z_2, Z_3, Z_4, \\ & Q_1 > 0, Q_2 > 0, Q_3 > 0, Q_4 > 0, \\ & \alpha > 0, \varepsilon > 0, \delta > 0 \\ & \text{or equivalently} \\ \left(-\dfrac{\alpha}{\beta}\mathrm{tr}P\right) \to & \inf \\ & P > 0, Z_1, Z_2, Z_3, Z_4, \\ & Q_1 > 0, Q_2 > 0, Q_3 > 0, Q_4 > 0, \\ & \alpha > 0, \varepsilon > 0, \delta > 0 \end{array} \tag{18}$$

subject the LMI's constraints (14). If the solutions P^*, Z_i^*, Q_i^* $\left(i = \overline{1,4}\right)$, α^*, ε^*, δ^* of this optimization problem are found, then the optimal parameters of the designed DNNO may be recuperated as

$$\begin{array}{c} L^* = (P^*)^{-1}Z_1^*,\ A^* = (P^*)^{-1}Z_2^*, \\ \mathring{W}_1^* = (P^*)^{-1}Z_3^*,\ \mathring{W}_2^* = (P^*)^{-1}Z_4^*. \end{array} \tag{19}$$

5.2 Algorithm of minimizing the attractive ellipsoid

Step 1. Chose appropriate $\Delta\alpha > 0$, $\Delta\varepsilon > 0$, $\Delta\delta > 0$, and $i = 1$.

Step 2. Find any values α_0, ε_0, δ_0 for which (18) has solution.

Step 3. Let $\alpha_i := \alpha_{i-1} + i\Delta\alpha$, $\varepsilon_i := \varepsilon_{i-1} - i\Delta\varepsilon$, $\delta_i := \delta_{i-1} - i\Delta\delta$. Solve the problem (18) for these values.

Step 4. If the solution exists, repeat Step 3 for $i := i+1$. If not, $\alpha^* := \alpha_{i-1}$, $\varepsilon^* := \varepsilon_{i-1}$, $\delta^* := \delta_{i-1}$, matrices P^*, Z_i^*, Q_i^* $\left(i = \overline{1,4}\right)$ are found from the solution of (18) for α^*, ε^*, δ^*.

$$\beta^* = 2\left\|\Lambda_x\right\|\left(\sum_{i=1}^{n}\left(x_i^+\right)^2 + \left(x^+\right)^2\right) + \left\|\Lambda_L\right\| v_+^2 + \varepsilon^*\theta + \left\|\Lambda_{\hat{w}_1}\right\|\left(L_{\Psi_1}^+\right)^2 + \left\|\Lambda_{\hat{w}_2}\right\|\left(L_{\Psi_2}^+ u_+\right)\Big)^2 + \left\|C\left(C^\top C + \delta^* I\right)^{-1}\Lambda_w\left(C^\top C + \delta I\right)^{-1}C^\top\right\|\left(v_+\right)^2.$$

6. EXPERIMENTAL EVALUATIONS

6.1 Materials

The compounds $Ce(NO_3)_3 \times 6H_2O$ (99%), $4-CPh$ (99%) and $4-PSA$ (99%) were used without further purification (Sigma–Aldrich). All the other reagents were analytical grade (J. T. Baker). The fixed initial concentration of all the contaminants ($4-CPh$ and $4-PSA$) was 100 mgL^{-1} and initial pH was fixed to 3.5. The pH parameter was not controlled during the ozonation.

6.2 Preparation of CeO_2 films

The selected catalyst (CeO_2) was deposed over clean glass slides as films. The supported catalyst, namely $CeO_2(f)$, was synthesized using an ultrasonic spray pyrolysis technique. The procedure initiated with a solution of cerium nitrate (0.6 gL^{-1}) which operated as precursor. The films of $CeO_2(f)$ were made over clean glass slides (LAUKA, $26.4 \times 76.2mm$) (Guzmán et al., 2020).

6.3 Catalyst evaluation on contaminant decomposition

Ozonation experiments for compounds $4-CPh$ and $4-PSA$ were carried out in a glass reactor (500 mL) with a porous filter at the bottom, which served as the ozone distributor to the liquid phase. Ozone was produced using an HTU500G generator fed with ultra-dried oxygen. The O_2-O_3 gas mixture flow (0.5 $Lmin^{-1}$) was limited by a mechanical rotameter. The input ozone concentration was (25 mgL^{-1}). The output ozone concentration was measured with a BMT 964 BT analyzer. In the experiments with the catalyst, the glass slides, coated with the CeO_2 film (an average of 1.64 mg in each film), were fixed in the reactor using a Teflon support (this material was selected considering its evident resistance against the oxidative power of ozone). The proposed reactor incorporates a fixed based to hold the glass slides distributed homogeneously around the reactor. This distribution was proposed with the aim of homogenize the contact between ozone and the catalyst films (Aguilar et al., 2016).

6.4 Analytical methods

The $4-CPh$ and $4-PSA$ concentrations were determined by high performance liquid chromatography (HPLC, Perkin Elmer, Flexar) with an array-diode detector. The C18 column (Nova Pack C18) was used in an isocratic mode with a mobile phase of water: acetonitrile (50 : 50 and 90 : 10 for $4-CPh$ and $4-PSA$, respectively) at 0.5 $mL \times min^{-1}$. In the case of oxalic acid, prevail organic acid column was used with KH_2PO_4 buffer solution at pH 2.5 (1.0 $ml\ min^{-1}$). All the experiments were done in triplicate.

6.5 Estimation results

The observer was applied considering that the ozone concentration at the reactor's output was the on-line available measure. The reconstructed information included the variation of the main contaminant. The application of the observer can be extended to include the variation of the byproducts' concentrations formed during ozonation, the dissolved oxygen in the aqueous phase in the reactor, as well as the concentration of hydroxyl radicals. In this study, we presented the reconstruction of the contaminants and their byproducts concentrations (of those identified compounds), which were considered the most valuable information for the practitioners.

The application of the optimization problem presented in subsection 5.1 yields the selection of the observer parameters. The optimization problem was numerically solved by implementing the algorithm proposed in this study with the aid of the Sedumi and Yalmip dual software. The entire algorithm was solved in the Matlab environment.

The parameters used for the projected DNN-observer evaluation were

$$A = diag\{[\,-0.25\ \ -0.34\ \ -1.24\ \ -1.26\,]\},$$
$$C = [\,1\ 0\ 0\ 0\,]^\top$$
$$P = \begin{bmatrix} 9.2 & 1.2 & -2.5 & -2.9 \\ 1.2 & 18.7 & 0.5 & 0.9 \\ -2.5 & 0.5 & 25.2 & -0.7 \\ -2.9 & 0.9 & -0.7 & 34.6 \end{bmatrix}$$
$$L = [\,26.1\ \ 15.7\ \ 22.4\ \ 18.2\,].$$

Matrix A was fixed from the beginning considering only the necessity of proposing such matrix as a Hurwitz one. Matrices P, and L were solved by the proposed numerical optimization algorithm described in subsection 5.1. Notice that such algorithm requires fixing values for α and β. The estimation of matrix P the following parameters $\alpha = 0.25$ and $\beta = 1.62 \times 10^{-2}$ were used. *Figure 1* depicts the comparison of the $4-CPh$ and $4-PSA$ concentrations obtained with the conventional, suspended and films-based catalytic ozonations, its non-projected estimation by the DNNO ($\bar{x}$) as well as the projected state ($\hat{x}$) are presented. This comparison does have a significant difference between the projected and non-projected state because the non-projected form yields the incorrect estimation of a negative concentration for the main contaminant. Such difference is remarkable indeed considering that the non-projected DNN has not information from the dynamics which can restrict the states evolution within the valid positive orthant.

The comparison of the byproduct's concentration formation and decomposition confirms the benefits of introducing the projection operator, because the estimated concentration is forced to be non-negative ($\hat{x}$) while the non-projected state detours to negative values (*Figure 2*).

The estimation of the root mean square error (RMSE) confirmed the significant differences of introducing the projection operator over the DNN observer. The magnitude of the RMSE for the non-projected case was 2 orders larger than the case for the projected case (*Figure 3*).

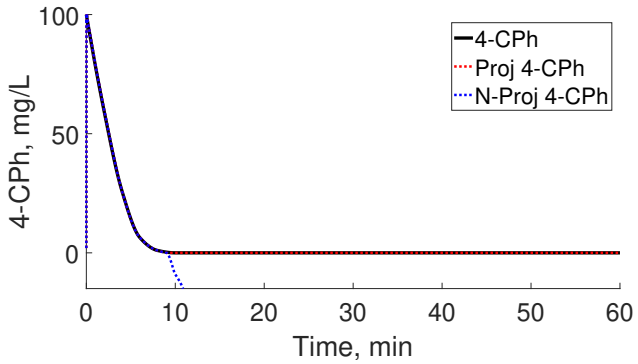

(a) 1-a

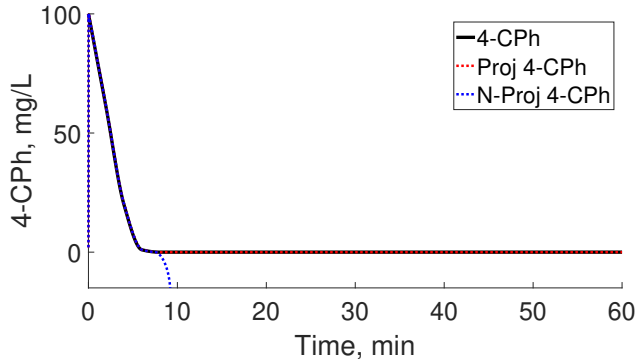

(b) 1-b

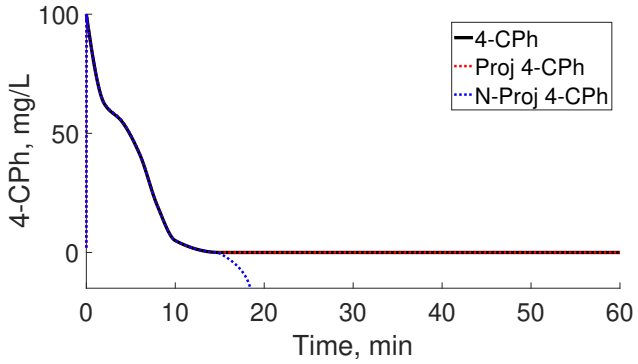

(c) 1-c

Fig. 1. Comparison of the estimated concentrations of 4-CP estimated with the projected and non-projected observer. a) Conventional, b) $CeO_2(s)$, c)$CeO_2(f)$.

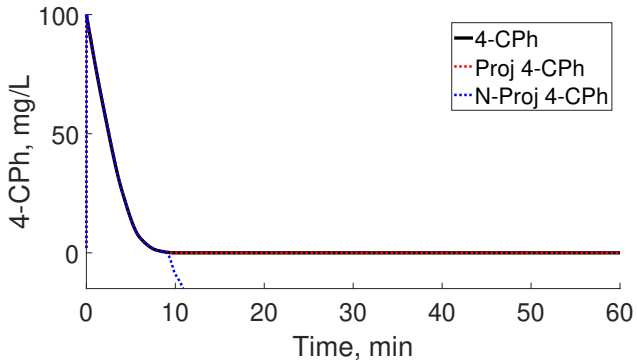

(a) 1-a

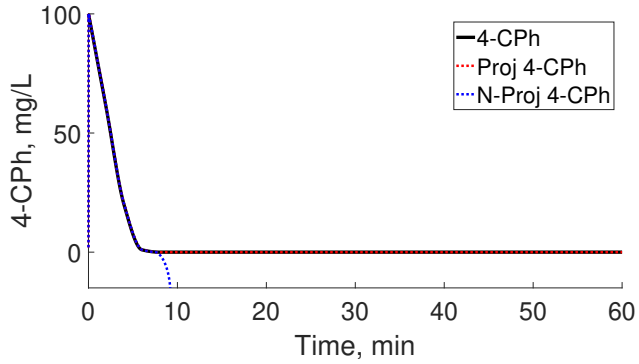

(b) 1-b

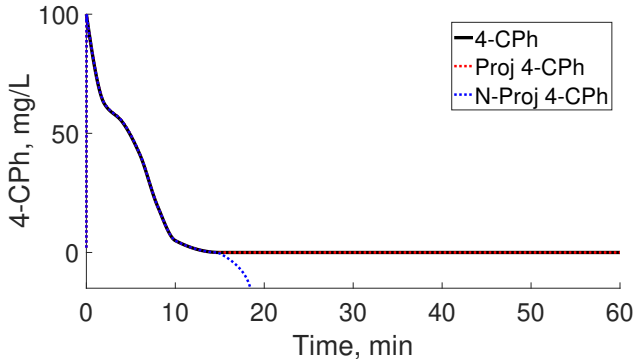

(c) 1-c

Fig. 2. Comparison of the estimated concentrations of the first byproduct obtained from 4-CP estimated with the projected and non-projected observer. a) Conventional, b) $CeO_2(s)$, c)$CeO_2(f)$.

7. CONCLUSIONS

This study considers the design of a new learning law for DNN, based on the application of a new variant of a projectional algorithm to estimate the states of a complex system, describing the ozonation of the toxic contaminant under the presence of the catalyst in two diverse variants: suspended and supported on thin films. The explicit idea of how to implement the projectional method in the continuous-time NN for estimating the variables of a positive system is described. The strict analysis for obtaining the upper bound of the method and to justify the asymptotic convergence of the estimation error is provided. The proposed method opens new researching opportunities to design a wide diversity of NN with a clear motivation on real plants.

REFERENCES

Aguilar, C., Rodriguez, J., Chairez, I., Galaviz, J., Vargas, J., and Poznyak, T. (2016). Naphthalene degradation in water/ethanol mixtures by catalytic ozonation based nickel oxide films. In *Abstracts of papers of the American chemical society*, volume 251. AMER CHEMICAL SOC 1155 16TH ST, NW, WASHINGTON, DC 20036 USA.

Chairez, I. (2009). Wavelet differential neural network observer. *IEEE Transactions on Neural Networks*, 20(9), 1439–1449.

Guan, Y.H., Ma, J., Ren, Y.M., Liu, Y.L., Xiao, J.Y., Lin, L.q., and Zhang, C. (2013). Efficient degradation of atrazine by magnetic porous copper ferrite catalyzed peroxymonosulfate oxidation via the formation of hydroxyl and sulfate radicals.

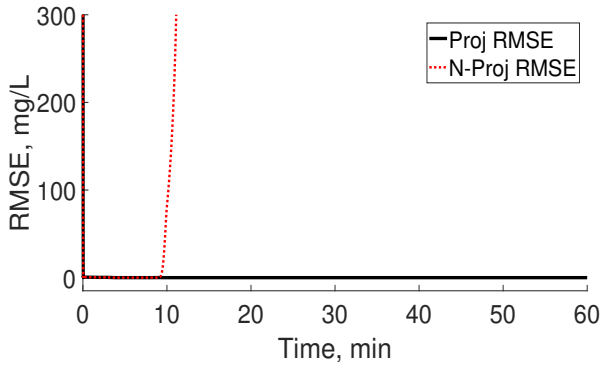

Fig. 3. Comparison of the estimated RMSE for the projected and non-projected observers..

.

Water research, 47(14), 5431–5438.

Guzmán, I.C., Rodríguez, J.L., Poznyak, T., Chairez, I., Hernández, I., and Hernández, R.T. (2020). Catalytic ozonation of 4-chlorophenol and 4-phenolsulfonic acid by ceo2 films. *Catalysis Communications*, 133, 105827.

Hassani, A., Khataee, A., Fathinia, M., and Karaca, S. (2018). Photocatalytic ozonation of ciprofloxacin from aqueous solution using tio2/mmt nanocomposite: Nonlinear modeling and optimization of the process via artificial neural network integrated genetic algorithm. *Process Safety and Environmental Protection*, 116, 365–376.

Li, L., Zhu, W., Zhang, P., Chen, Z., and Han, W. (2003). Photocatalytic oxidation and ozonation of catechol over carbon-black-modified nano-tio2 thin films supported on al sheet. *Water Research*, 37(15), 3646–3651.

Nawrocki, J. and Kasprzyk-Hordern, B. (2010). The efficiency and mechanisms of catalytic ozonation. *Applied Catalysis B: Environmental*, 99(1-2), 27–42.

Poznyak, A., Sanchez, E., and Yu, W. (2001). *Differential Neural Networks for Robust Nonlinear Control (Identification, State Estimation and Trajectory Tracking)*. World Scientific.

Poznyak, A. (2009). *Advanced Mathematical Tools for Automatic Control Engineers. Vol. I. Deterministic Systems.* Springer.

Poznyak, T., Chairez, I., and Poznyak, A. (2019a). Output-based modeling of catalytic ozonation by differential neural networks with discontinuous learning law. *Process Safety and Environmental Protection*, 122, 83–93.

Poznyak, T., Chairez, I., and Poznyak, A. (2019b). *Ozonation and Biodegradation in Environmental Engineering: Dynamic Neural Network Approach*. Elsevier, 1st edition.

Rodríguez, J.L., Poznyak, T., Valenzuela, M.A., Tiznado, H., and Chairez, I. (2013). Surface interactions and mechanistic studies of 2, 4-dichlorophenoxyacetic acid degradation by catalytic ozonation in presence of ni/tio2. *Chemical engineering journal*, 222, 426–434.

Wang, J. and Bai, Z. (2017). Fe-based catalysts for heterogeneous catalytic ozonation of emerging contaminants in water and wastewater. *Chemical Engineering Journal*, 312, 79–98.

Wu, J. (1998). Symmetric functional differential equations and neural networks with memory. *Transactions of the American mathematical society*, 350(12), 4799–4838.

APPENDIX

Proof. Consider the Lyapunov-like function

$$V_P(t) = \|\bar{x}(t) - x(t)\|_P^2 + \sum_{i=1}^{2} k_{w,i} \mathrm{tr}\left\{\tilde{W}_i^\top(t)\tilde{W}_i(t)\right\} \tag{20}$$

and define the vectors $\Delta := \bar{x}(t) - x(t)$ and $e(t) = C\bar{x}(t) - y(t)$ for which we have

$$\begin{aligned} e(t) &= C\bar{x}(t) - y(t) = C\Delta(t) - \nu(t), \\ \Delta(t) &= \left(C^\top C + \delta I\right)^{-1} C^\top e(t) + w(t), \\ w(t) &:= \left(C^\top C + \delta I\right)^{-1} \left[\delta I \Delta + C^\top \nu(t)\right]. \end{aligned} \tag{21}$$

Differentiation of (20) on the trajectories of the system gives

$$\begin{gathered} \dot{V}_P(t) = S(t) + S_1(t) + S_{11}(t) + \\ +2\left[\bar{x}(t) - x(t)\right]^\top P\left[(A - LC)\left(\bar{x}(t) - x(t)\right)\right] \\ -2\left[\bar{x}(t) - x(t)\right]^\top P\delta_A f(x,u,t) \end{gathered}$$

where

$$\begin{aligned} S(t) &:= 2\sum_{i=1}^{2} k_{w,i} \mathrm{tr}\left\{\tilde{W}_i^\top(t)\dot{W}_i(t)\right\} + \\ &2\left[e^\top C\left(C^\top C + \delta I\right)^{-1} + w^\top(t)\right] PW_1(t)\Psi_1(\hat{x}(t)), \\ &2\left[e^\top C\left(C^\top C + \delta I\right)^{-1} + w^\top(t)\right] PW_2(t)\Psi_2(\hat{x}(t))u(t) \\ S_1(t) &:= 2\left[\bar{x}(t) - x(t)\right]^\top P(A - LC)\left(\hat{x}(t) - \bar{x}(t)\right), \\ S_{11}(t) &:= 2\left[\bar{x}(t) - x(t)\right]^\top PL\nu(t). \end{aligned}$$

In view of the Λ-inequality (see Lemma 12.1 in Poznyak (2009)) the following upper estimates for the derivative of the Lyapunov-like function holds:

$$\begin{aligned} &\dot{V}_P(t) \le \varpi^\top \tilde{H}(P, L, A \mid \alpha, \varepsilon)\varpi - \\ &\alpha\|\bar{x}(t) - x(t)\|_P^2 + S(t) + \beta_2, \\ &\beta_1 := 2\|\Lambda_x\|\left(\sum_{i=1}^{n}\left(x_i^+\right)^2 + \left(x^+\right)^2\right) + \\ &\|\Lambda_L\| v_+^2,\ \beta_2 := \beta_1 + \varepsilon\theta, \\ &\varpi = \begin{bmatrix} \bar{x}(t) - x(t) \\ \delta_A f(x,u,t) \end{bmatrix} \end{aligned}$$

with $\tilde{H}(P, L, A \mid \alpha, \varepsilon) := \begin{pmatrix} \tilde{H}_{11} & -P \\ -P & -\varepsilon I_{n\times n} \end{pmatrix}$. Here

$$\begin{gathered} \tilde{H}_{11} = P(A - LC) + (A - LC)^\top P + \\ P(A - LC)\Lambda_x^{-1}(A - LC)^\top P + \alpha P + \\ 2\|\Lambda_x\| I_{n\times n} + PL\Lambda_L^{-1}L^\top P \end{gathered}$$

. In view of Learning Laws (12)

$$\begin{aligned} &\mathrm{tr}\left\{2\tilde{W}_1^\top(t)P\left(C^\top C + \delta I\right)^{-1} C^\top e\Psi_1^\top(\hat{x}(t))\right\} + \\ &\mathrm{tr}\left\{2\tilde{W}_2^\top(t)P\left(C^\top C + \delta I\right)^{-1} C^\top eu^\top(t)\Psi_2^\top(\hat{x}(t))\right\} + \\ &\mathrm{tr}\left\{\tilde{W}_1^\top(t)P\Lambda_w^{-1}P\tilde{W}_1(t)\Psi_1(\hat{x}(t))\Psi_1^\top(\hat{x}(t))\right\} + \\ &\mathrm{tr}\left\{\tilde{W}_2^\top(t)P\Lambda_w^{-1}P\tilde{W}_2(t)\Psi_2(\hat{x}(t))u(t)\cdot\right. \\ &\left. u^\top(t)\Psi_2^\top(\hat{x}(t))\right\} + 2\sum_{i=1}^{2} k_{w,i}\mathrm{tr}\left\{\tilde{W}_i^\top(t)\dot{W}_i(t)\right\} + \\ &\alpha\sum_{i=1}^{2} k_{w,i}\mathrm{tr}\left\{\tilde{W}_i^\top(t)\tilde{W}_i(t)\right\} = 0 \end{aligned}$$

and in view of the property (14), one gets $\dot{V}_P(t) \le -\alpha V_P(t) + \beta$ implying

$$V_P(t) \le \left[V_P(0) + \frac{\beta}{\alpha}\right] e^{-\alpha t} + \frac{\beta}{\alpha}.$$

By (11),

$$\begin{aligned} \limsup_{t\to\infty} \|\hat{x}(t) - x(t)\|_P^2 &\le \limsup_{t\to\infty} \|\bar{x}(t) - x(t)\|_P^2 \\ &\le \limsup_{t\to\infty} V_P(t) \le \frac{\beta}{\alpha} \end{aligned}$$

which is equivalent to (15). □